Desalination and Water Treatment
www.deswater.com
doi: 10.5004/dwt.2020.25387

184 (2020) 57–71
April

Thermodynamic analysis of multi effect desalination unit with thermal vapor compression feed by different motive steam pressures

Ighball Baniasad Askari[a,*], Mehran Ameri[b]

[a]*Department of Mechanical Engineering, Faculty of Engineering, University of Zabol, Sistan and Baluchestan, Iran, email: eghball.baniasad@uoz.ac.ir*
[b]*Department of Mechanical Engineering, Faculty of Engineering, Shahid Bahonar University of Kerman, Kerman, Iran, email: ameri_mm@uk.ac.ir*

Received 9 July 2019; Accepted 22 December 2019

ABSTRACT

The previous research works have proven that the location of the thermal vapor compression (TVC) plays an important role on the performance of the multi effect desalination (MED) plant. The objective of this paper is to investigate the effects of different design parameters such as TVC location, motive steam pressure, seawater temperature, number of effects (N_{eff}s), and heating steam temperatures on gain output ratio (GOR), specific energy consumption and exergy efficiency (η_{ex}) of the system. Since wide ranges of design parameters were considered, the results are helpful for primary design and best operation modes of the MED/TVC plant when it is located at different places across the world. The results revealed that for each N_{eff}s, there is an optimal location for TVC to obtain the maximum GOR, maximum η_{ex}, and minimum specific heat transfer area (SA). For lower N_{eff}s, the optimum TVC location is less affected by motive steam pressure. However, by increasing the N_{eff}s, the optimum TVC location is shifted to the upper effects. Also, the η_{ex} and SA were shown to be changed between 3.5% and 7%, and 450 and 900 m^2/(kg/s), respectively.

Keywords: Thermal desalination; MED; Thermal vapor compression; Thermodynamic analysis

1. Introduction

The Persian Gulf seawater with the salinity of 46,000 ppm [1,2] is a great water source for countries such as Iran, Saudi Arabia, Qatar, United Arab Emirates, and Bahrain to provide their fresh water requirements through the desalination plants. A comprehensive review of the water desalination technology in Iran [3] shows that among 38 desalination plants that are installed in Iran, the multi-stage flash (MSF), multi effect desalination (MED), and RO production capacity shares are nearly equal to 8%, 33%, and 59%, respectively. The MED technology consumes less energy than the MSF. As compared with RO, which produces fresh water with approximately 200 ppm, the MED fresh water is salt-free due to the evaporation–condensation process. The application of the thermal vapor compression (TVC) unit in the MED system results in higher gain output ratios (GORs) for the whole system over the MED system [4]. The MED unit benefits the low-grade heat sources with heating temperatures of ranges from 55°C to 110°C. Therefore, MED can be integrated into the other energy systems such as the absorption chillers [5], the absorption heat pumps, the vapor-compression refrigeration systems [6] and heat pumps [7], or it can be replaced by the condenser of the Rankine cycles [8,9].

MED/TVC requires high-pressure vapor that can be directly provided by different thermal sources such as fossil fuels [10], concentrated solar fields [11], the vapor stream extracted from the steam turbine of the Rankine cycle power plants [12], and the high-grade waste heat of the gas turbine or supercritical CO_2 Brayton cycles [13].

According to the literature, there are many studies concerning the MED/TVC thermodynamic analysis. For

* Corresponding author.

instance, a steady-state mathematical model of the MED/TVC system with different N_{eff}s (4–12 numbers) was developed by Bin Amer [14]. The optimum operational conditions of the system were determined based on the optimum values for top brine temperature as well as the compression and entrainment ratios of the TVC unit. The GOR of the system was determined as a value between 8.5 and 18.5. Also, it was shown that the specific heat transfer area, the entrainment ratio (Ra, the entrained steam mass flow rate per unit of motive steam mass flow rate), and GOR are increased by increasing the N_{eff}s.

Al-Mutaz and Wazeer [15] investigated the MED/TVC unit to determine the effect of different parameters on the performance of the system with different N_{eff}s (4–12 numbers). They showed that the system with 4 and 12 effects has the GOR of 7.34 and 15.04, respectively. Besides, the results of that study showed that the entrainment ratio and GOR would be increased by increasing the N_{eff}s while the specific heat consumption is decreased.

The thermodynamic analysis of the MED/TVC system locating the TVC after different effects has been rarely investigated. Alasfour et al. [16] performed a thermodynamic analysis for three different MED/TVC configurations with six effects. In two configurations, the TVC is located after the last and third effects. The formulations of first and second laws of thermodynamics were applied to determine the influence of different parameters on the performances of three configurations of the study. It was found that the TVC and effects have the most portions of exergy destruction among the other components of the system. Besides, with decrease in motive steam pressure, the decrease in exergy efficiency is higher than that in the GOR of the system.

Ortega-Delgado et al. [17] performed a parametric study on the MED/TVC unit. The effects of motive and suction steam pressures on the performance of the system were investigated for a MED/TVC unit with 12 effects, and the motive steam pressures of 362–4,540 kPa. It was concluded that at higher motive steam pressures, the TVC should be located closer to the last effect. Also, for high electricity demand, the motive steam should be low and TVC should be located close to the 5th effect, and for low electricity demand, the motive steam pressure should be high and the TVC should be located closer to the last effect. Besides, the highest GOR of the plant (14.66) was obtained for the motive steam pressure of 4,540 kPa.

A five-effect MED/TVC system without the feed water heaters and flashing boxes was considered by Kouhikamali et al. [18]. The influence of changing the TVC location on the amount of energy consumption of the system was investigated in that work. It was shown that the changing of the TVC from the last effect to the middle effects results in a considerable increase in the entrainment ratio and consequently, it causes to decrease the energy consumption of the system. That research was performed for top brine and cooling seawater temperatures of 64°C and 30°C, respectively, and for motive steam pressures of 500; 1,200, and 2,000 kPa.

Fathia et al. [19] investigated a double effect MED/TVC system which is integrated with a thermal power plant in a phosphoric acid factory for a water production rate of 528 m^3/d. An exergo-economic analysis and a multi-objective optimization method were performed to determine the optimum configuration of the system yielding the maximum exergy efficiency and minimum water production cost. The results of that study showed that TVC has the major exergy destruction among the other components of the system. Also, the exergy efficiency of the MED/TVC was obtained as 2.24% for the motive steam pressures of between 450 and 650 kPa.

Khalid et al. [20] performed a mathematical method to determine the optimum location of the TVC in the forward feed and parallel feed MED/TVC systems with 4–12 effects. The performance ratio (PR) of the desalination plant was determined at different design parameters such as the total heat transfer surface area of the plant and the cooling water flow rate. The authors of that study concluded that locating the TVC at the middle effect results in higher PRs and lower specific seawater flow rates. Also, for motive steam pressures of between 200 and 3,500 kPa, the maximum PR of the system was obtained at the motive steam pressure of 1,500 kPa.

Elsayed et al. [21] used an exergo-economic model for evaluating different MED configurations (backward feed, forward feed, parallel feed, and parallel cross feed with the TVC unit). The better performance parameters were obtained for the parallel cross feed configuration. However, this configuration was shown to have the highest specific cooling seawater flow rate. The exergy efficiency of the system was determined as a value between 4% and 6% for different motive steam pressures ranging from 300 to 2,400 kPa.

Based on the literature, as concerned to our knowledge, few studies address the thermodynamic analysis of the MED/TVC desalination system. For example, the effect of changing the TVC location on the performance of the system has been investigated only in the study by Ortega-Delgado et al. [17], Kouhikamali et al. [18], Khalid et al. [20]. However, the results that are presented in these references are associated with the system with a specific cooling seawater temperature. Besides, in the study by Ortega-Delgado et al. [17] and Kouhikamali et al. [18], the calculations were performed only for 12 and 5 effects, respectively.

The main goal of the present study is to perform a comprehensive thermodynamic analysis of the MED/TVC system aiming at the determination of the optimum location of the TVC to obtain the highest GORs and second law efficiencies. The novelty is that unlike the previous studies, which are associated with specific N_{eff}s, motive steam pressures or seawater temperatures, the described system in the present study was considered for different N_{eff}s (8–16 numbers) and wide ranges of the motive steam pressure (250–4,540 kPa), the heating steam temperature (65°C–80°C), and the seawater temperature (21°C–36°C). Therefore, the results could be helpful for the primary design of MED-TVC plants located at different places across the world working at different operational conditions. The influences of different design parameters such as cooling seawater temperature, heating steam temperature, motive steam pressure and TVC location in the GOR, the specific heat transfer area, the heat consumption, and the entrainment ratio of the desalination unit were investigated using energy analysis. Also, the specific exergy destruction and exergy efficiency of the system were considered changing different design parameters of the system. This research is the first part of a bigger project and will be followed by exergo-economic analysis of the MED/TVC system integrated to the Rankine and gas turbine power plants powered by renewable and different non-renewable thermal sources.

2. Method and thermodynamic modeling

The main components of a parallel feed MED/TVC desalination unit are evaporators (effects), steam ejector or TVC, condenser, feed water heaters, flashing boxes, distillate and brine pumps as well as the water intake pumps as can be seen in Fig. 1. The low pressure vapor (D_r) called as entrained vapor is taken from one of the effects as the motive steam (D_s) with high pressure enters into the TVC unit. After the mixing of motive steam and entrained vapor, the resultant vapor with an intermediate pressure (D_d, discharged vapor) exits from the TVC unit and flows into the MED first effect. The discharged vapor delivers its latent heat into the first effect of the MED and leaves that at the saturated liquid state; part of which is returned into the boiler (D_s) and the rest (D_r) is flowed into the flashing boxes and finally joins the distilled water pipeline. A small fraction of D_r (shown by "y") is flashed in each flashing boxes and then joins the output vapor of the corresponding effect (D_1 to D_n) to be flowed into the feed water heaters, warms up the feed water and then is used as the heating steam of the next effect. The condenser is used to cool down the vapor that is generated in the last effect. Part of the intake seawater is used as the feed water and the other part is returned to the sea. The feed water is divided into equal streams to be sprayed into the effects. The brine is flowed from each effect to the next one and finally, it is introduced into a plate heat exchanger using the brine pump. The brine and distillate plate heat exchangers are used to cool down the distilled water and brine exiting the MED.

The mass and energy balance equations for each component of the system were used in the thermodynamic modeling of the MED/TVC unit. A computer program was developed in MATLAB to determine different parameters such as the total heat transfer area, amount of distillate, intake seawater and feed water mass flow rates, temperature at each effect and some other performance parameters such as GOR, specific heat consumption (SHC), specific exergy destruction (SED) and exergy efficiency (η_{ex}) of the desalination plant.

The following assumptions were considered in modeling of the system [4,17,22]:

- The seawater salinity was set as 46000 ppm according to Persian Gulf seawater salinity [1,2,4].
- The temperature difference between the effects and feed water heaters are the same.
- Heat losses from the equipment to the surrounding are not considered [17].
- The processes in the TVC part are adiabatic.
- The processes were considered to have steady state conditions.
- The first effect feed water is set as 56°C and the last effect feed water temperature is 2°C less than its heating temperature.
- The temperature losses due to pressure drop of the vapor in demisters, connecting lines and inside evaporators are neglected. [21]
- The heating vapor entering and leaving the effects, the motive and entrained vapors are assumed to be saturated [17].

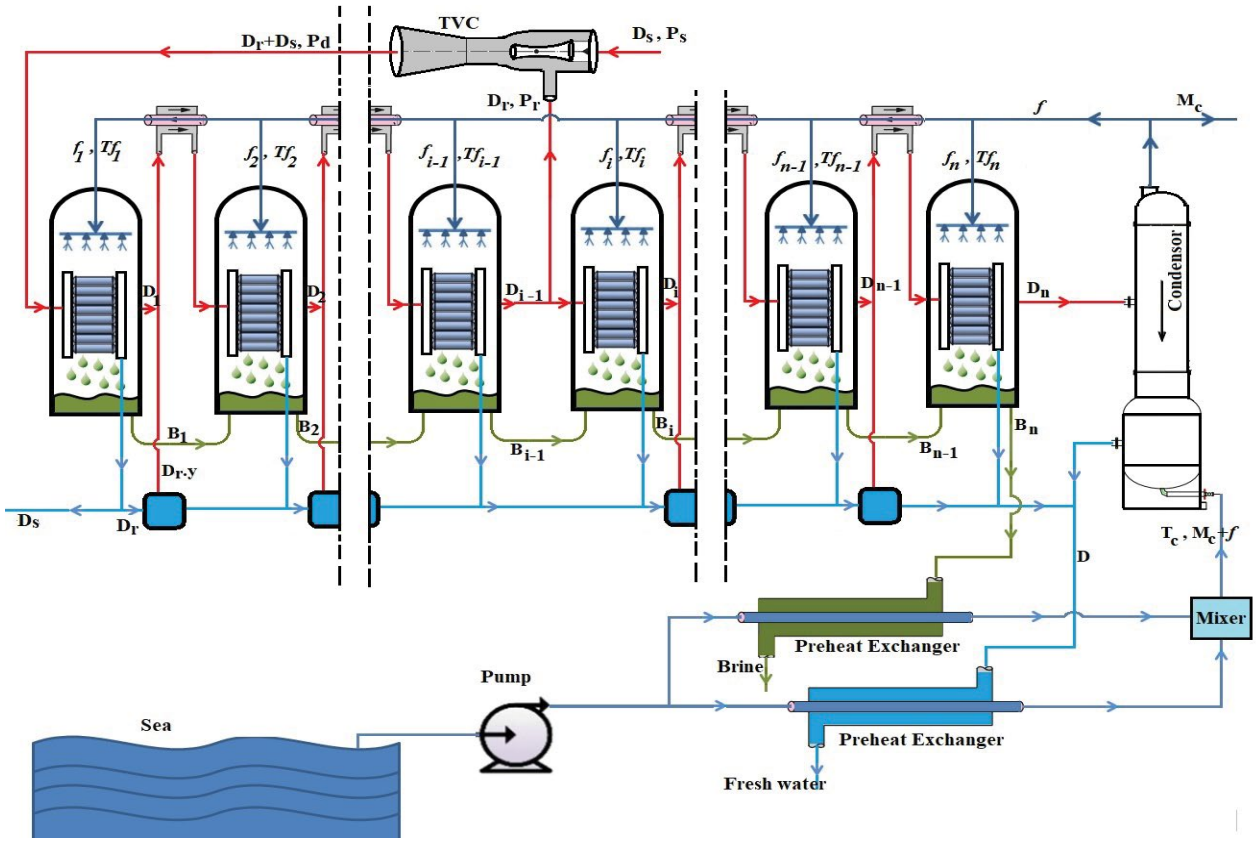

Fig. 1. MED/TVC system-parallel feed.

- The resultant distillate is free of salt [23].
- The temperature difference of 9°C was considered between the input and output streams in the condenser.
- The temperature drops in the first effect is equal to 2.5°C.
- The seawater concentration at the output was considered as 69500ppm [17].

The calculations were performed for four different heating steam temperatures of 65°C, 70°C, 75°C, and 80°C. Also, three seawater temperatures of 21°C, 26°C, 31°C, and 36°C were considered in the calculations. The thermo-physical properties of the pure water and steam were acquired using a subprogram called "Xsteam" which is freely available and operates as a MATLAB script. The MALAB code includes 13 inputs such as the heating steam temperature, motive steam flowrate, number of effects, seawater temperature, the effectiveness of heat exchangers, input and output salinity of seawater and so forth. Also, 15 parameters were obtained as the outputs of the MATLAB program including, the GOR, amount of distillate, the temperatures of the effects, specific heat transfer area, seawater mass flow rate, exergy efficiency and etc. Three loops were used in the MATLAB code to calculate the thermodynamic formulations associated with the effects before the TVC location, the effect with TVC, and the other effects after the TVC. The calculations were allowed to be checked for the constraints such as salinity of the brine at each effect and the temperature difference between the effects.

The following formulations were applied in the thermodynamic analysis of the MED/TVC unit [14,15]:

2.1. Formulations which are same for different effects, condenser, feed water heaters, and flashing boxes

The temperature of each effect was determined based on the first and last effect temperatures as well as the N_{eff}s:

$$T_{i+1} = T_i - \Delta T_{\text{eff}} \tag{1}$$

ΔT_{eff} is the temperature drop in the effects which was considered to be the same for all effects:

$$\Delta T_{\text{eff}} = \frac{T_1 - T_n}{n-1} \tag{2}$$

Saturation temperature of effects:

$$T_{\text{vi}} = T_i - \text{BPE} - \text{NEA} \tag{3}$$

where the BPE is the amount of increase in boiling temperature because the presence of dissolved salt in the water [24], and NEA is the efficiency of the flashing process:

$$\begin{gathered}\text{BPE} = \alpha \times S^2 + \beta \times S \\ \left\{\begin{gathered}\alpha = -4.854 \times 10^{-4} \times T^2 + 2.823 \times 10^{-1} \times T + 17.95 \\ \beta = 1.536 \times 10^{-4} \times T^2 + 5.267 \times 10^{-2} \times T + 6.56\end{gathered}\right\}\end{gathered} \tag{4}$$

The above equation is valid for the temperature (T) range of 0°C to 200°C and seawater salinity (S) of 0 to 120 kg/kg. It is worth mentioning that 120 kg/kg is equal to 1,20,000 ppm.

$$\text{NEA}_i = \frac{33 \cdot \left(T_{i-1} - T_i\right)^{0.55}}{\text{Tv}_i} \qquad i = 2,3,\ldots,N \tag{5}$$

The fraction of the condensed vapor that is flashed when it is directed to the flashing box was calculated using the following equation:

$$y_i = \frac{C \cdot \Delta T_{\text{eff}}}{\lambda_i} \tag{6}$$

where C is the specific heat and λ is the latent heat of the evaporation that can be obtained as follows:

$$\begin{aligned}\lambda = {} & 2,501.897149 - 2.407064037 \times T + \\ & 1.192217 \times 10^{-3} \times T^2 - 1.5863 \times 10^{-5} \times T^3\end{aligned} \tag{7}$$

The overall heat transfer coefficient for effects [15]:

$$U_e = \frac{1,939.4 + 1.40562T_i - 0.0207525(T_i)^2 + 0.0023186(T_i)^3}{1,000} \tag{8}$$

Feed water preheater heat transfer areas:

$$A_{\text{fi}} = \frac{C \cdot \Delta T_{\text{fi}} \cdot \sum_{k=1}^{i} F_k}{U_f \cdot \left(T_{\text{fi}} - T_{\text{fi+1}}\right)} \cdot \ln\left[\frac{T_{\text{vi}} - T_{\text{fi+1}}}{T_{\text{vi}} - T_{\text{fi}}}\right] \tag{9}$$

where F_k is the feed water mass flow rate in effect kth.

2.2. First effect

The brine is directed from each effect to the next effect. The amount of brine in each effect is determined based on the feed water mass flow rate (F) and distillate mass flow rate of that effect:

$$B_1 = F_1 - D_1 \tag{10}$$

where the amount of feed water is equal for each effect and it is calculated using the total feed water mass flow rate and N_{eff}s:

$$F_j = \frac{F}{n} \tag{11}$$

The amount of vapor generated in first effect is calculated as follows:

$$D_1 = \frac{\left[\left(D_s + D_r\right) \cdot \left(h_d - h_{\text{fd}}\right)\right]}{\lambda_1} - F_1 \cdot C \cdot \left(\frac{T_1 - T_{f1}}{\lambda_1}\right) \tag{12}$$

where λ_1 is the latent heat of evaporation in the first effect (kJ/kg). Also, D_r and D_s are the entrained vapor and motive steam mass flow rates, respectively.

The heat transfer area for each effect was calculated as follows:

$$A_{e1} = \frac{\left[\left(D_s + D_r\right) \cdot \left(h_d - h_{\text{fd}}\right)\right]}{U_{e1} \cdot \left(T_d - T_1\right)} \tag{13}$$

Brine salinity leaving the first effect:

$$X_{b1} = \frac{F_1}{F_1 - D_1} \cdot X_f \tag{14}$$

2.2. Second effect to i–1th effect (TVC location) (k = 2 to i–1)

Brine mass balance:

$$B_j = \sum_{j=1}^{j=n} F_j - D_j \tag{15}$$

Heating vapor:

$$D_k = \left[\left(D_{k-1} + (\sum_{k=1}^{k-2} D_k + D_r)\cdot y - (k-1)\cdot F_k \cdot y\right)\right]\cdot \frac{\lambda_{k-1}}{\lambda_k} - F_k \cdot C \cdot \left(\frac{T_k - T_{\text{fk}}}{\lambda_k}\right) + B_{k-1}\cdot \frac{C\cdot \Delta T}{\lambda_k} \tag{16}$$

Heat transfer area:

$$A_{\text{ek}-1} = \frac{\left[\left(D_{k-2} + (\sum_{k=1}^{k-3} D_k + D_r)\cdot y - (k-2)\cdot F_k \cdot y\right)\right]\cdot \lambda_{k-2}}{U_{\text{ek}-1}\cdot (T_{\text{vk}-2} - T_{k-1})} \tag{17}$$

Brine salinity living the effect:

$$X_{\text{bi}+1} = \frac{X_f \cdot F_{i+1}}{\sum_{i=1}^{i+1}(F_i - D_i)} \tag{18}$$

2.3. First effect after TVC location (ith)

Heating vapor:

$$D_i = D_f \cdot \frac{\lambda_{i-1}}{\lambda_i} - F_i \cdot C \cdot \left(\frac{T_i - T_{\text{fi}}}{\lambda_i}\right) + B_{i-1}\cdot \frac{C.\Delta T}{\lambda_i} \tag{19}$$

Heat transfer area:

$$A_{\text{ei}} = \frac{D_f \cdot \lambda_{i-1}}{U_{\text{ei}}\cdot (T_{\text{vi}-1} - T_i)} \tag{20}$$

2.4. Second effect to last effect after TVC location (k = i + 1 to n)

Heating vapor:

$$D_i = \left[\left(D_{i-1} + \sum_{i=1}^{i-2} D_i \cdot y - (i-1)\cdot F_i \cdot y\right)\right]\cdot \frac{\lambda_{i-1}}{\lambda_i} - F_i \cdot C \cdot \left(\frac{T_i - T_{\text{fi}}}{\lambda_i}\right) + B_i \cdot \frac{C\cdot \Delta T}{\lambda_i} \tag{21}$$

Heat transfer area:

$$A_{\text{ei}} = \frac{\left[\left(D_{i-1} + \sum_{i=1}^{i-2} D_i \cdot y - (i-1)\cdot F_i \cdot y\right)\right]\cdot \lambda_{i-1}}{U_{\text{ei}}\cdot (T_{\text{vi}-1} - T_i)} \tag{22}$$

2.5. Condenser

Heat transfer area:

$$A_c = \frac{D_n \cdot \lambda_n}{U_c \cdot (\text{LMTD})_c} \tag{23}$$

Logarithmic mean temperature difference:

$$(\text{LMTD})_c = \frac{(T_{\text{vn}} - T_f) - (T_{\text{vn}} - T_c)}{\ln\left[\frac{T_{\text{vn}} - T_f}{T_{\text{vn}} - T_c}\right]} \tag{24}$$

Overall heat transfer coefficient [15]:

$$U_c = 1.7194 + 3.2063\cdot 10^{-2}\cdot T_{\text{vn}} - 1.5971\cdot 10^{-5}\cdot (T_{\text{vn}})^2 + 1.9918\cdot 10^{-7}\cdot (T_{\text{vn}})^3 \tag{25}$$

Cooling seawater flowing through the condenser:

$$M_c = \frac{D_n \cdot \lambda_n}{C\cdot (T_n - T_c)} \tag{26}$$

2.6. Thermo-compressor

Entrainment ratio or mixing ratio [12,25]:

$$R_a = \frac{D_s}{D_r} = a_1 + a_2\cdot C_r + \frac{a_3}{E_r} + a_4\cdot C_r^2 + \frac{a_5}{E_r^2} + a_6\cdot \frac{C_r}{E_r} + a_7\cdot C_r^3 + \frac{a_8}{E_r^3} + a_9\cdot \frac{C_r}{E_r^2} + a_{10}\cdot \frac{C_r^2}{E_r} \tag{27}$$

Please refer to Table 1 for constants of the above equation. In the above equation, D_s and D_r are the motive steam and entrained vapor mass flow rates, respectively (Fig. 1).

Compression ratio is the ratio of discharge pressure to the entrained pressure:

$$C_r = \frac{P_d}{P_r} \tag{28}$$

Table 1
Constants of the polynomial model adopted for TVC performance [25]

Constant	$10 \le E_r \le 100$	$E_r \ge 100$
a1	–3.20842211	–1.93422581
a2	3.933353	2.152524
a3	27.236	113.4909
a4	–1.19206949	–0.52222106
a5	–141.42328825	–14,735.96533618
a6	–22.54551842	–31.85197010
a7	0.125813	0.047507
a8	348.5066	900,786
a9	41.7961	–495.58154134
a10	4.439929	10.02513

where subscripts *s*, *r*, and *d* represent the motive steam, entrained vapor, and discharged vapor, respectively.

Expansion ratio:

$$E_r = \frac{P_s}{P_r} \tag{29}$$

2.7. Performance parameters

GOR is the ratio of distillate mass flow rate to the motive steam mass flow rate:

$$\text{GOR} = \frac{D}{D_s} \tag{30}$$

Specific heat transfer area is the ratio of the MED/TVC total heat transfer areas (effects, condenser, and preheaters) to the distillate mass flow rate (m^2/(kg/s)).

$$\text{SA} = \frac{\left(\sum_{i=1}^{i=n} A_e + A_c + \sum_{i=1}^{i=n-1} A_{\text{fi}}\right)}{D} \tag{31}$$

Specific heat consumption is the amount of thermal energy that is consumed to produce each kg of the distillate (kJ/kg):

$$\text{SHC} = \frac{D_s \cdot \lambda_s}{D} \tag{32}$$

2.8. Exergy efficiency and total exergy destruction of MED/TVC

Exergy balances can be written considering the sole physical exergy related to the material and energy streams entering and exiting the system.

$$\text{ex} = \left(h - h_o\right) - T_o \times \left(s - s_o\right) \tag{33}$$

where T_0, h_0, and s_0, respectively, indicate the temperature enthalpy and entropy of the considered dead state (T = 25°C, P = 101.3 kPa). The chemical exergy of fresh water can be determined based on the minimum theoretical work of separation required in the desalination process as follows [4,12,26,27]:

$$\dot{E}_{\text{fresh}} = \dot{N}^{\text{fresh}} \times \varnothing \times R_u \times T_0 \times X_{s,\text{feed}} \tag{34}$$

where $\dot{N}^{\text{fresh}}$ is the molar flow rate of product freshwater that is defined as follows:

$$\dot{N}_{\text{Fresh}} = \frac{\dot{m}_{\text{fresh}}}{\text{MM}_{\text{water}}} \tag{35}$$

where R_u is the universal constant of gases, $\varnothing$ is the dissociation factor of salts, $X_{s,\text{feed}}$ is the molar fraction of the dissolved salts, and MM_{water} is the molar weight of water (18 kg/kmol). Please refer to the study by Calise et al. [26,27] for further information. All the required expressions for energy and exergy analysis were implemented MATLAB. The MED/TVC inlet and outlet exergy streams are shown in Fig. 2. As can be seen, the inlet exergy streams include the seawater, MED/TVC required electricity and the motive steam exergy flow rate. Also, the fresh water, brine, and part of the preheated seawater that exceeds the required feed seawater are included in the outlet exergy streams. The outlet seawater and the rejected brine are not useful. Also, the intake seawater stream has no cost and is free. Therefore, the exergy efficiency of the system could be calculated based on the fuels (electricity and motive steam) and useful products (fresh water) of the system [12]. The exergy efficiency of the MED/TVC unit was calculated based on the input heating motive steam exergy (EX_s), required electricity work in the MED unit ($\dot{W}_{\text{MED/TVC}}$) and output exergy of the fresh water as follows:

$$\eta_{\text{ex}} = \frac{\dot{E}_{\text{fresh}}}{\left(E\dot{X}_s + \dot{W}_{\text{MED/TVC}}\right)} \tag{36}$$

$\dot{W}_{\text{MED/TVC}}$ is the total electricity consumption by the MED/TVC, which is calculated considering the specific electricity consumption of 1.55 kWh/m^3 for the plant [28].

$$E\dot{X}_s = \dot{m}_s \times \left(\left(h_s - h_o\right) - T_o \times \left(s_s - s_o\right)\right) \tag{37}$$

where $\dot{m}_s$ and h_s are the motive steam mass flow rate and enthalpy, respectively. The specific exergy destruction was calculated using the following equation:

$$\text{SED} = \frac{E\dot{X}_s + \dot{W}_{\text{MED/TVC}} - \dot{E}_{\text{fresh}}}{D} \tag{38}$$

3. Model validation

For the first, the accuracy of the model was validated by making a comparison between the results of the present model and that are reported in the study by Ortega-Delgado et al. [17]. As it is tabulated in Table 2, the performance parameters of GOR, SA and optimum TVC location that

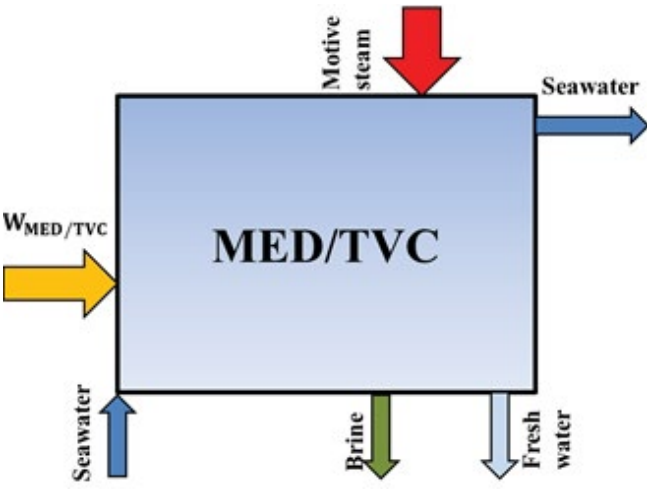

Fig. 2. Block diagram of MED/TVC with the input and output exergy streams.

Table 2
Comparison between the present study and the experimental data obtained from Trapani desalination unit

Input variables	Reference [17]	Model
Number of effects (N_{eff}s)	12	12
Seawater salinity (ppm)	40,000	40,000
Seawater concentration at output (ppm)	65,900	65,900
Motive pressure P_s, kPa	4,540	4,540
Seawater cooling temperature (T_{SW}) (°C)	25.9	25.9
Motive steam temperature(T_{MS}) (°C)	70	70
Top brine temperature (T_1), (°C)	–	67.5
Minimum brine temperature (T_n), (°C)	37	37
Feed seawater temperature to nth effect (T_f), (°C)	35	35
Feed seawater temperature to 1st effect (T_{f1}), (°C)	60	60
Results		
Temperature drop per effect, (ΔT)	2.7–2.8	2.77
Optimum effect for TVC location	11	11
GOR	14.66	15.00
SA (m^2/[kg/s of distillate])	523.46	520.52

are obtained from the calculations of the present work are in good agreement with that are addressed in the study by Ortega-Delgado et al. [17].

4. Results and discussions

As stated formerly, the thermodynamic formulations were used in MATLAB to determine the amount of brine, distillate, salinity of brine, heating vapor generated at each effect as well as the performance parameters of the system. The effects of increasing the seawater temperature, heating steam temperature and pressure, N_{eff}s and temperature difference between the effects on the GOR, exergy efficiency, SHC, SED were investigated. The optimum TVC location for different N_{eff}s was found in this part of the study.

4.1. Effect of motive steam pressure

Different motive steam pressures of 250, 362, 450, 800, 2,000, and 4,540 kPa which are commonly used in the MED/TVC water desalination technology were considered in the present study. As stated in the introduction section, the required motive steam is usually extracted from the steam turbine of the fossil fuel, nuclear or solar thermal Rankine cycle power plants, gas turbine stack heat recovery or it is directly generated in a fossil fuel boiler or concentrated solar field. Fig. 3 shows the variation in GOR of the system for the motive steam pressure of 250 kPa, seawater temperature of 26°C, heating discharge steam temperature of 70°C and different N_{eff}s from 8 to 16 numbers. As can be seen from Fig. 3, for each N_{eff}s in a specific TVC location, the GOR of the system would be maximized. For instance, for 8 and 16 effects, the maximum GOR is obtained for the TVC located in effects 5 and 12, respectively. The shifting of the optimum TVC location to the upper effects when increasing the motive steam pressure could be explained by the GOR definition (Eq. (30)). The decreasing of the motive steam mass flow rate or increasing the distillate mass flow rate results in increasing the GOR. At higher motive steam pressures (P_s), the vapor could be entrained at lower suction pressures (P_r, TVC is located closer to the last effect) using a low motive steam mass flow rate to reach specific conditions at the TVC outlet. When the motive steam pressure is decreased from higher to lower values (from 4,540 to 250 kPa), the motive steam mass flow rate should be increased to entrain the vapor. Therefore, to decrease the exploitation of energy by vapor recompression, the TVC location should be shifted to the effects further from the last effect to increase the suction pressure and consequently to entrain more amount of vapor using lower motive steam mass flow rates. Fig. 4 shows the variation trend of the GOR at different motive steam pressure and N_{eff}s. As clear from Fig. 4, the GOR of system with 16 effects is increased from 16.2 to 18.8 (16% increase) with increasing the motive steam pressure from 250 to 4,540 kPa. By increasing the N_{eff}s and considering constant heating steam and seawater temperatures of, respectively, 70°C and 26°C, the temperature difference between the effects would be decreased. The increasing of the motive steam pressure and decreasing of temperature difference between the effects results in shifting the TVC location from the middle effects to the effects closer to the last effects. As it is seen in Fig. 4, for 14 effects, the TVC optimum location is changed from the effect 10th to 13th by increasing the motive steam pressure from 250 to 4,540 kPa, respectively. Also, for 12 effects, the increase of the motive steam pressure from 800 to 4,540 kPa would result in changing the optimum TVC location from the effect 9th to 11th, respectively.

It is evident that the increasing of effect numbers in the MED/TVC system results in increasing the heat transfer area and consequently system capital costs. Figs. 5 and 6 show the specific heat transfer area (SA) of the MED/TVC unit for system with 10 and 16 effects, respectively, at three different motive steam pressures. As can be seen, by changing the TVC location from the middle effects to the upper effects, the SA of the system is increased. By increasing of motive steam pressure, a small decrease can be achieved in the SA of the

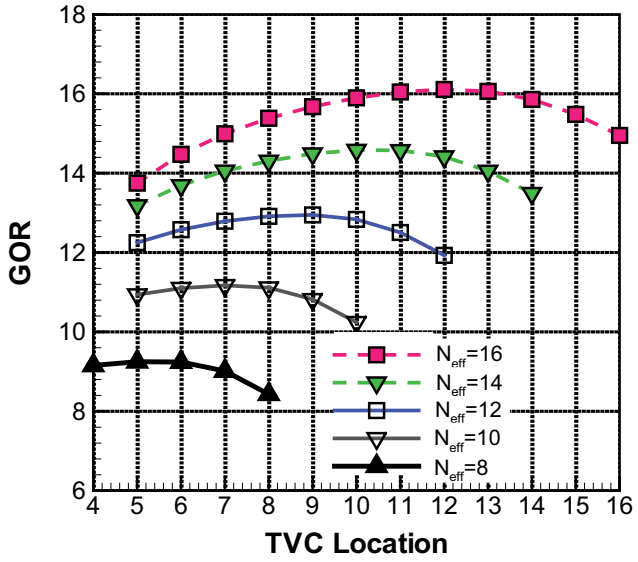

Fig. 3. Variation of GOR and TVC location with N_{eff}s. T_{SW} = 26°C, T_S = 70°C, P_m = 250 kPa.

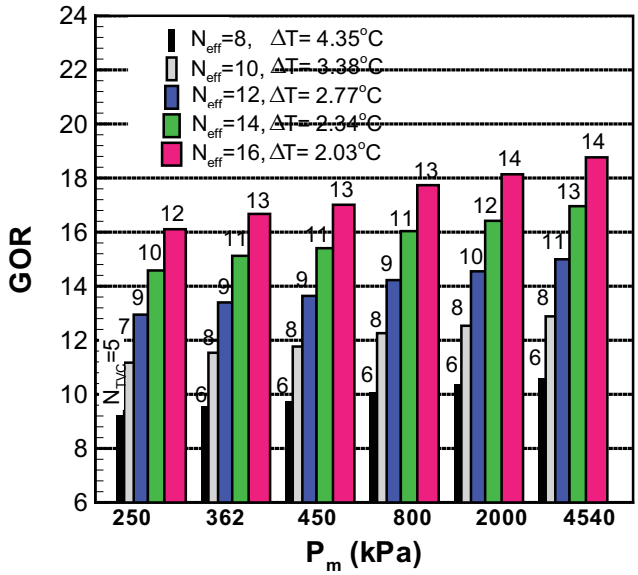

Fig. 4. Variation of GOR and TVC location with motive steam pressure. T_{SW} = 26°C, T_S = 70°C.

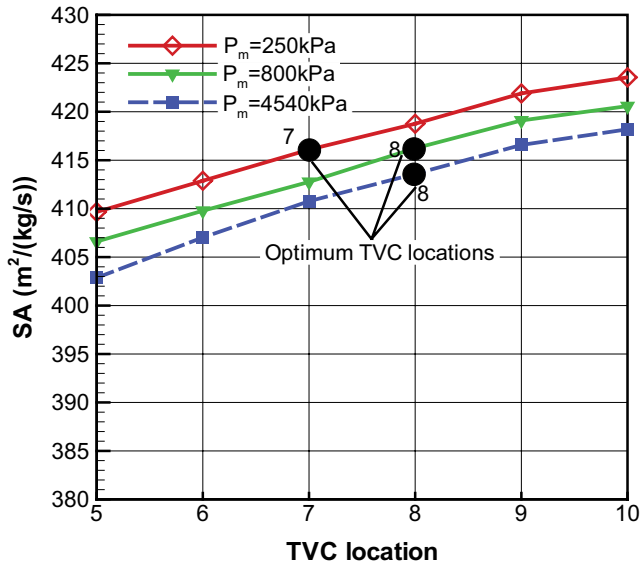

Fig. 5. Specific heat transfer area vs. TVC location and motive steam pressure, 10 effects, T_{SW} = 26°C, T_S = 70°C.

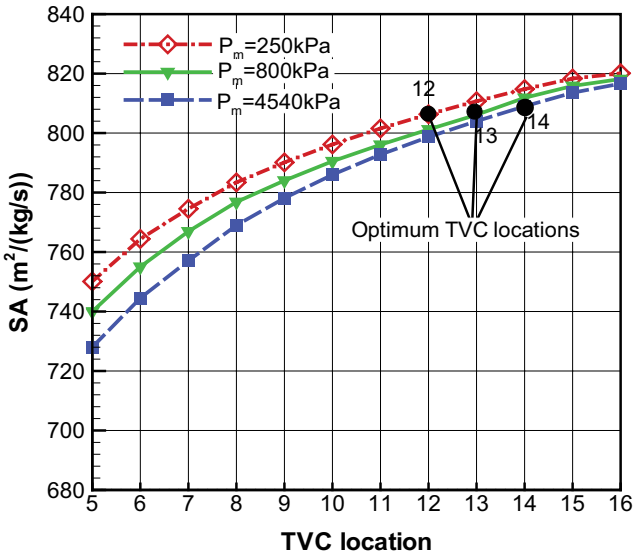

Fig. 6. Specific heat transfer area vs. TVC location and motive steam pressure, 16 effects, T_{SW} = 26°C, T_S = 70°C.

system. The optimum TVC locations yielding the maximum GOR are also shown in Figs. 5 and 6; where it is clear that the SA of the system is approximately equal to the same value for different motive steam pressures when the TVC located in the optimal location. For instance, the SA of the system with the optimum TVC location is nearly equal to 414 and 814 m²/(kg/s) for 10 and 16 effects, respectively.

Fig. 7 shows that for all motive steam pressures, the SA of the system is increased from 300 to 800 m²/(kg/s) (166% increase) by increasing the N_{eff}s from 8 to 16 numbers (two-fold increase). For 10, 12, and 14 effects, the SA would be obtained as 414, 523, and 658 m²/(kg/s), respectively. For 12 effects, the results of Fig. 7 are in a good agreement with that is reported in the study by Ortega-Delgado et al. [17]. Please see Table 2 for the operating conditions and assumptions that were used in the validation of the present model with the results shown in the study by Ortega-Delgado et al. [17].

As mentioned formerly, the entrainment ratio is the ratio between the motive steam and suction steam mass flow rates (Ra, Eq. (27)). Fig. 8 shows the variation of Ra with TVC location for MED/TVC unit with different N_{eff}s and motive steam pressure of 250 kPa. As can be seen, Ra is increased by shifting the TVC location from the middle effects to the last effect. In other words, Ra would be increased by decreasing the suction pressure. In fact, the decreasing of suction pressure results in decreasing the entrained vapor mass flow rate. As

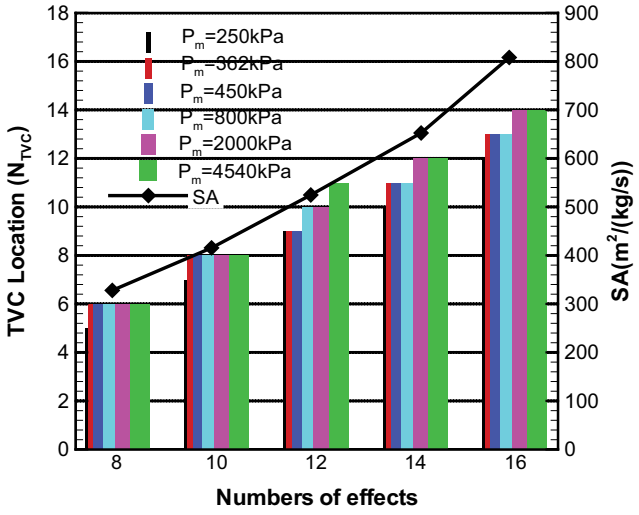

Fig. 7. Effect of N_{eff}s on specific heat transfer area and optimal TVC location. T_{SW} = 26°C, T_S = 70°C.

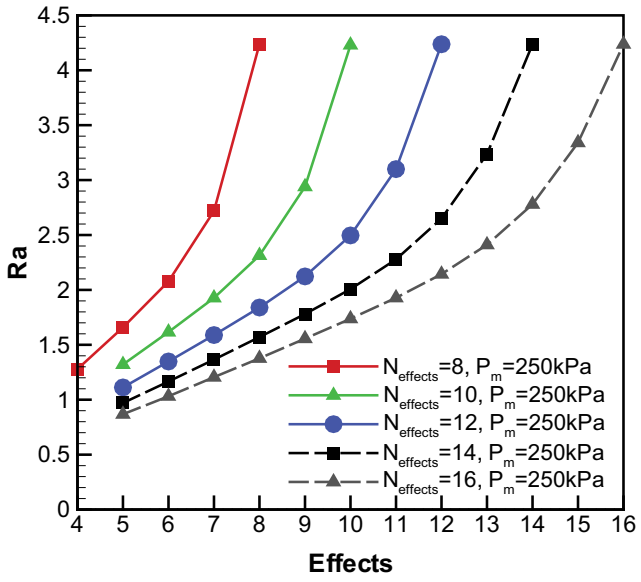

Fig. 8. Effect of N_{eff}s on the entrainment ratio, T_{SW} = 26°C, T_S = 70°C.

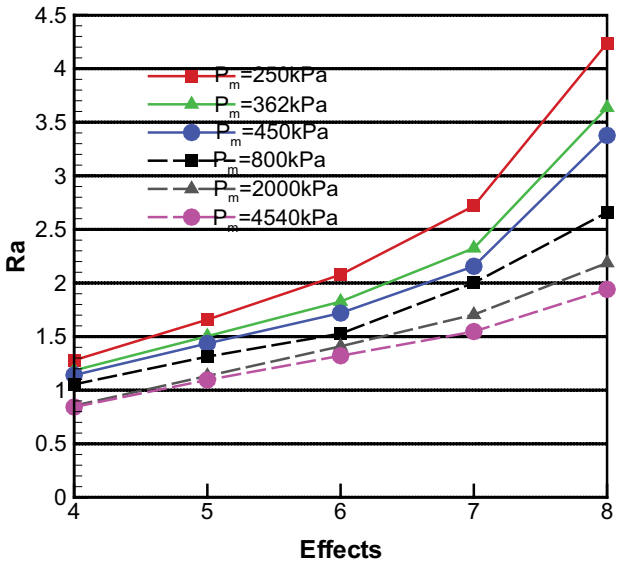

Fig. 9. Effect of motive steam pressure on the entrainment ratio of system with eight effects. T_{SW} = 26°C, T_S = 70°C.

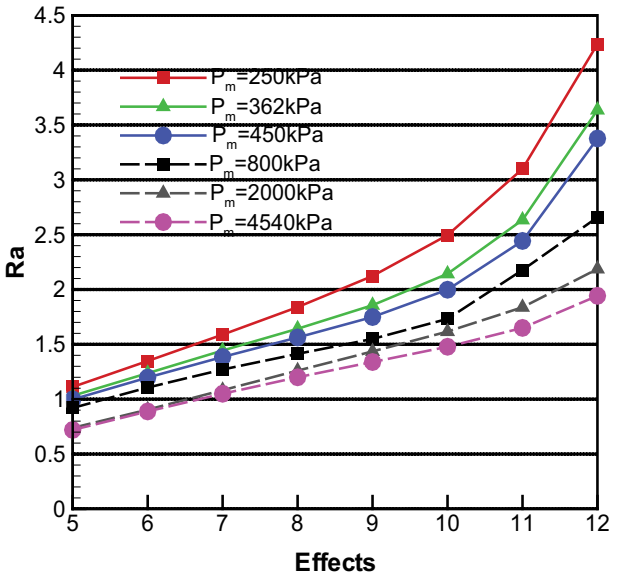

Fig. 10. Effect of motive steam pressure on the entrainment ratio of system with 12 effects. T_{SW} = 26°C, T_S = 70°C.

a consequence, to have a certain condition at TVC outlet, the motive steam mass flow rate should be increased (increasing the Ra).

The effect of motive steam pressure on the entrainment ratios of the MED/TVC unit with 8, 12, and 16 effects is shown in Figs. 9–11, respectively, for seawater temperature of 26°C and heating steam temperature of 70°C. As can be seen from Figs. 9–11, the increasing of motive steam pressure decreases the Ra for the fixed TVC location. In fact, the higher motive steam pressures lead to higher suction vapor mass flow rates and as the consequence to lower the motive steam mass flow rates. It is worth to mention that for the optimum TVC locations (Fig. 7), by increasing the N_{eff}s from 8 (TVC in effect 6th) to 16 numbers (TVC in effect 12th), Ra changes from 1.65 to 2.14 and from 1.32 to 1.56 for motive steam pressures of 250 and 4,540 kPa, respectively, as it is depicted in Figs. 9 and 11. Because T_{SW} and consequently the temperature of the last effect ($T(n)$) was considered to be the same for different effect numbers, the entrained vapor pressure (P_r, Eq. (29)) for the TVC in the last effect is equal to the same value. That is why for each motive steam pressure in Figs. 9–11, the Ra for the TVC located in the last effect is obtained to be equal based on Eqs. (27)–(29).

Fig. 12 shows the variation of SHC with the motive steam pressure for the MED/TVC unit with two different effect numbers of 10 and 14 numbers by applying Eq. (32). Generally, the increasing of motive steam pressure results in decreasing the SHC for each number of effects. Fig. 12

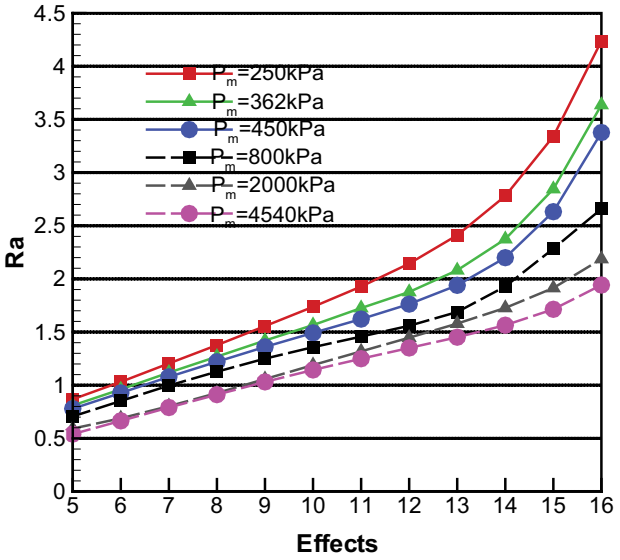

Fig. 11. Effect of motive steam pressure on the entrainment ratio of system with 16 effects. T_{SW} = 26°C, T_S = 70°C.

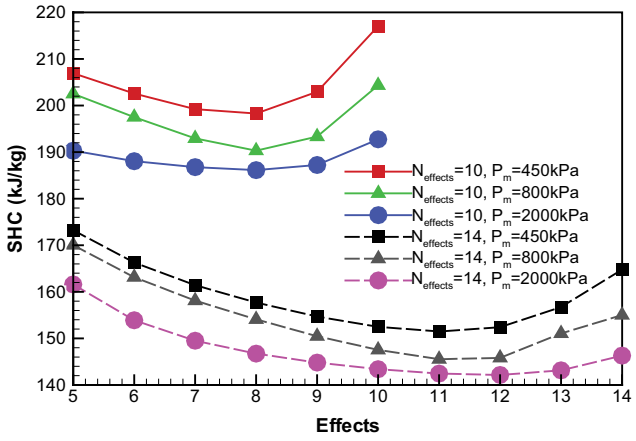

Fig. 12. Effect of motive steam pressure on the specific heat consumption of system with 10 and 14 effects, T_{SW} = 26°C, T_S = 70°C.

also determines that at each motive steam pressure, the minimum SHC is obtained at the optimum TVC location (Fig. 7). Also, it can be observed from Fig. 12 that increasing the number of effects from 10 to 14 numbers results in decreasing the SHC of the system by about 31% for different motive steam pressures. The results also show that for the MED/TVC system with motive steam pressure of 4,540 kPa with 8 and 16 effects, the minimum SHC of system is obtained as 219 and 124 kJ/kg, respectively. It is worth to mention that making a decision about increasing the N_{eff}s to decrease the SHC is depended on both the motive steam price and the MED evaporator capital costs. For instance, the results of Figs. 7 and 12 show that the increase of the N_{eff}s from 10 to 14 numbers results in increasing the SA by about 62.5% and decreasing the SHC by about 31%. Therefore, whether the increase in the N_{eff}s is efficient or not is a trade-off between the energy efficiency and the capital costs of the system.

Figs. 13 and 14 show the exergy efficiency (η_{ex}) and the SED of the MED/TVC system for 8 and 14 numbers of effects, respectively. It is clear from these figures that the increasing of motive steam pressure results in increasing the SED and consequently decreasing the exergy efficiency of the system. For each motive steam pressure, the minimum SED (and maximum exergy efficiency) is obtained for the systems with optimum TVC locations (Fig. 7). The results also show that the exergy efficiency of the system with motive steam pressure of 4,540 kPa changes from 5.03% to 5.42% by increasing the numbers of effects from 8 to 16 numbers. It is worth mentioning that a low value for the exergy efficiency of the MED/TVC system was also reported in the study by Catrini et al. [12], where for the specific seawater temperature of 26°C and salinity of 38,000 ppm, the exergy efficiency of the MED/TVC unit with 12 effects was obtained as 7.1% and 4.95%, for the motive steam pressures of 290 and 4,890 kPa, respectively.

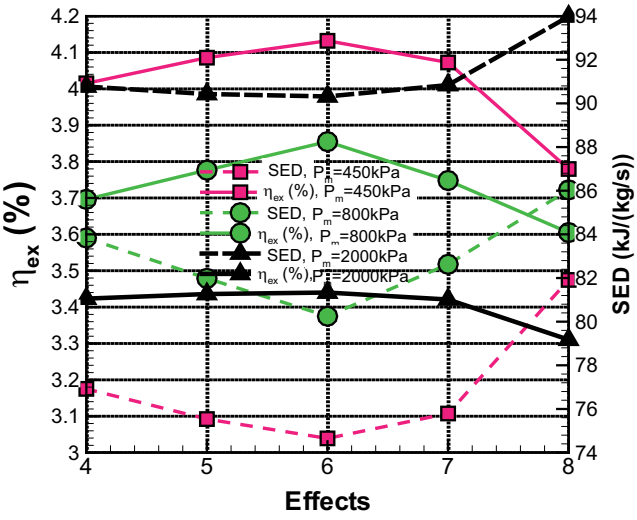

Fig. 13. Effect of motive steam pressure on the specific exergy destruction and exergy efficiency of system with eight effects, T_{SW} = 26°C, T_S = 70°C.

4.2. Effect of heating steam temperature (T_S)

One of the parameters that affect the performance of the MED/TVC system is the heating steam temperature. The heating steam temperature was assumed to be 2.5°C higher than the top brine temperature at the first effect. In this section, for a MED/TVC unit feeding with a cooling seawater temperature of 26°C and having 12 numbers of effects, the heating steam temperature of the system was changed from 65°C to 80°C and the effect of this increase on the system performance parameters was considered. Fig. 15 shows that the increase in the heating steam temperature leads to an increase in the temperature difference between the effects (ΔT_{eff}) and to decrease the GOR of the system for different motive steam pressures. In fact, the increasing of the ΔT_{eff} causes to increase the TVC discharge pressure (C_r, Eq. (28)), and this requires an extra motive steam mass flow rate. As a consequence, the GOR of the system is decreased by increasing the heating steam temperature.

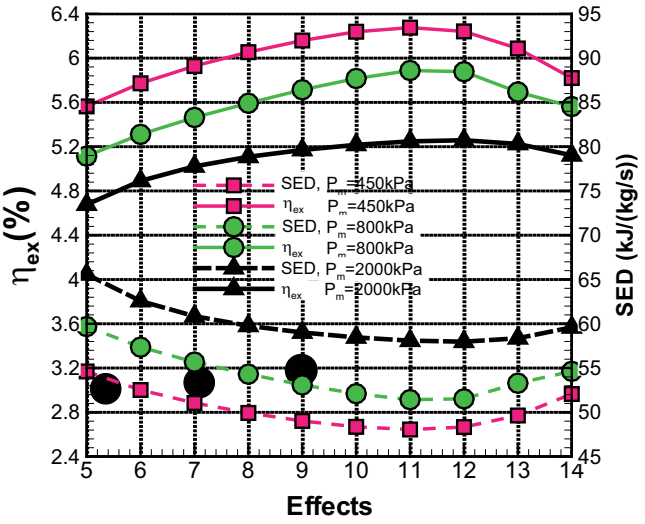

Fig. 14. Effect of motive steam pressure on the specific exergy destruction and exergy efficiency of system with 14 effects, T_{SW} = 26°C, T_S = 70°C.

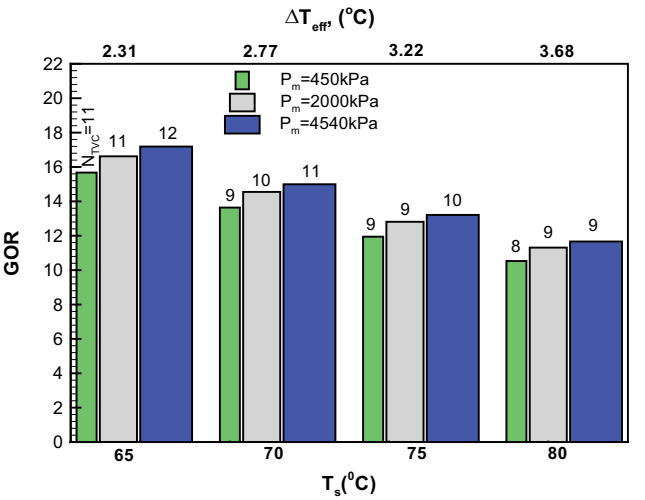

Fig. 15. Effect of motive steam pressure on the GOR of system, 12 effects, T_{SW} = 26°C.

As was mentioned in the explanations of Figs. 5 and 6, the SA of the MED/TVC system with a specific effect number and for the TVC placed at its optimum location approaches the same value at different motive steam pressures. The average SA of the system for different N_{eff}s is shown in Fig. 16. As can be seen, the increasing of the heating steam temperature results in decreasing the SA of the system. The reason is that the increasing of ΔT_{eff}, which happened because of the increasing of heating steam temperature, results in increasing the overall heat transfer coefficient and consequently decreasing the specific heat transfer area (Eqs. (5), (11), (18), and (20)). Since ΔT_{eff} is considered as the driven force of the evaporation process, the lower heat transfer area is required when ΔT_{eff} is increased.

The impact of heating steam temperature in the specific heat consumption of the system is shown in Fig. 17. This figure shows that the SHC of the system increases by increasing the T_S. In fact, the increase in ΔT_{eff}, which is followed by

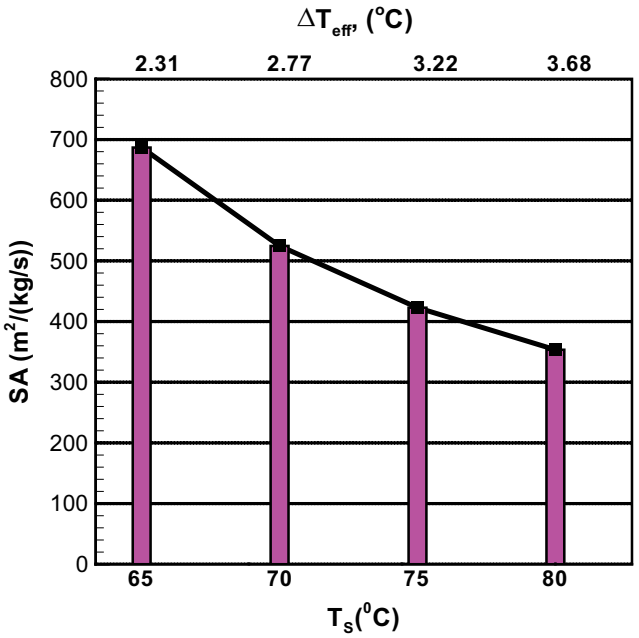

Fig. 16. Effect of motive steam pressure on the specific heat transfer area of system, 12 effects, T_{SW} = 26°C.

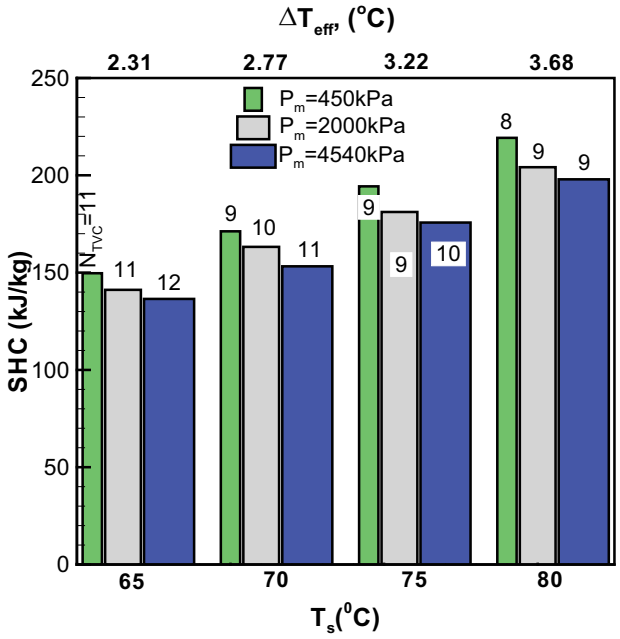

Fig. 17. Effect of motive steam pressure on the SHC of system, 12 effects, T_{SW} = 26°C.

decreasing the SA, decreases the GOR values (Fig. 15) and consequently increases the SHC of the system (Fig. 17). Also, Fig. 17 shows that the increase of the motive steam pressure results in decrease in the SHC at each heating steam temperature for the system with 12 effects and TVC located at the optimum location yielding the highest GORs. The variation of specific exergy destruction and exergy efficiency of the MED/TVC system with increasing the T_S is shown in Fig. 18. As can be seen, the increasing of T_S causes decrease

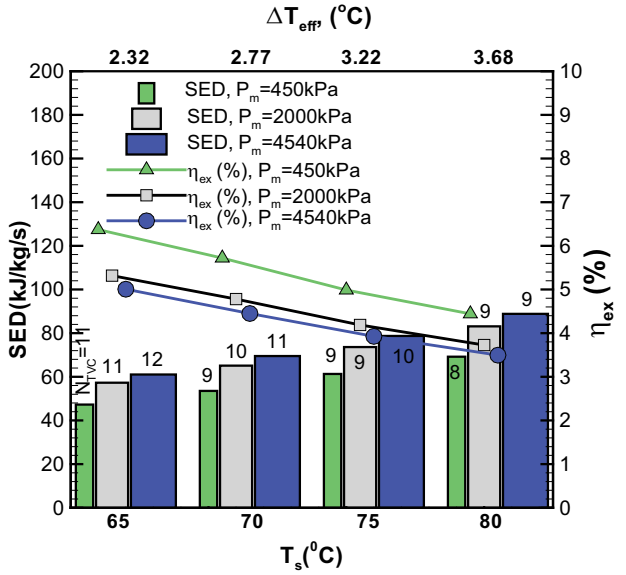

Fig. 18. Effect of motive steam pressure on the SED and Ex_{eff} of the system, 12 effects, T_{SW} = 26°C.

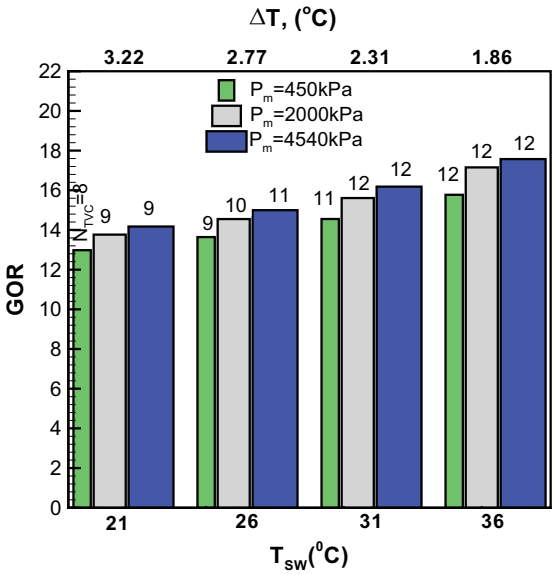

Fig. 19. Effect of cooling seawater temperature on the GOR of system, 12 effects, T_S = 70°C.

in the exergy efficiency of the system. The reason is that the increase of the ΔT_{eff} results in increase of the TVC discharge pressure (C_r), which leads to high irreversibilities. It is obvious that the system with highest SED has the lowest exergy efficiency. Therefore, the higher heating steam temperatures, the system has the lower exergy efficiencies.

4.3. Effect of cooling seawater temperature (T_{SW})

In practice, the cooling seawater inlet temperature in the condenser changes during the year time and can affect the feed water temperature that is sprayed on the effects. In this part of the study, the effect of cooling seawater temperature on the GOR, specific heat transfer area (SA), SHC, SED, and exergy efficiency of the system was investigated. Fig. 19 shows the effect of T_{SW} on GOR of the MED/TVC system with 12 effects, the constant heating steam temperature of T_S = 70°C and three different motive steam pressures. As it can be seen from Fig. 19, the increasing of cooling seawater temperature leads to increasing the GOR of the system. The reason is that the increasing of T_{SW} results in increasing the feed water temperature (T_f), and feed water with higher temperatures needs lower heat to be preheated as can be seen in Fig. 20. Therefore, the lower the specific heat consumption the higher the GOR. The results of Fig. 19 show that each 10°C increase in the T_{SW} leads to 13% increase in GOR of the system. Fig. 19 also shows that for the system with specific motive steam pressures, by increasing the T_{SW}, the optimum location of TVC shifts from the middle effects to the later effects. For instance, for the motive steam of 4,540 kPa, the optimum TVC location at T_{SW} = 21°C is in effect 9th which is changed to the effect 12th by increasing the T_{SW} to 36°C. In fact, the increasing of T_{SW} results in decreasing of the ΔT_{eff}, which causes to decrease the TVC discharge pressure (C_r). The decreasing of TVC discharge pressure leads to shifting the optimum TVC location to the upper effects and also decreasing the amount of required motive steam mass flow rate. In consequence, the

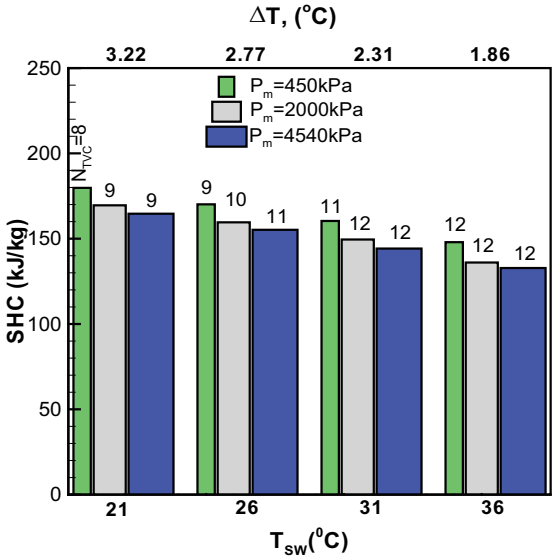

Fig. 20. Effect of cooling seawater temperature on the SHC of system, 12 effects, T_S = 70°C.

GOR of the system would be increased. Fig. 20 also shows that the SHC of the system would be decreased by about 16% by 10°C increase in the cooling seawater temperature. The average required specific heat transfer area for the MED/TVC unit with 12 effects and heating steam temperature of 70°C is shown in Fig. 21 for different cooling seawater temperatures. As can be seen in this figure, at a constant heating steam temperature, the increasing of cooling sweater temperature results in decreasing the ΔT_{eff} and consequently decreasing the overall heat transfer coefficient. The lower the overall heat transfer coefficient the higher the SA. Fig. 21 also shows that the increase of T_{SW} from 21°C to 26°C, from 26°C to 31°C and from 31°C to 36°C, results in increasing the SA of the system by 18%, 23%, and 40%, respectively. The increasing

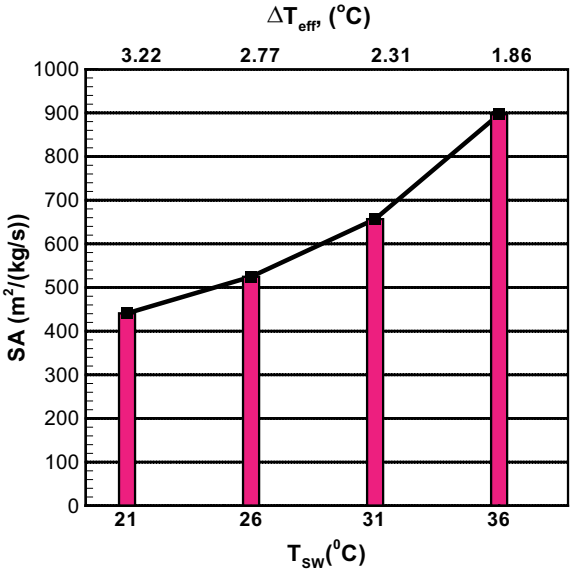

Fig. 21. Effect of cooling seawater temperature on the SA of system, 12 effects, T_S = 70°C.

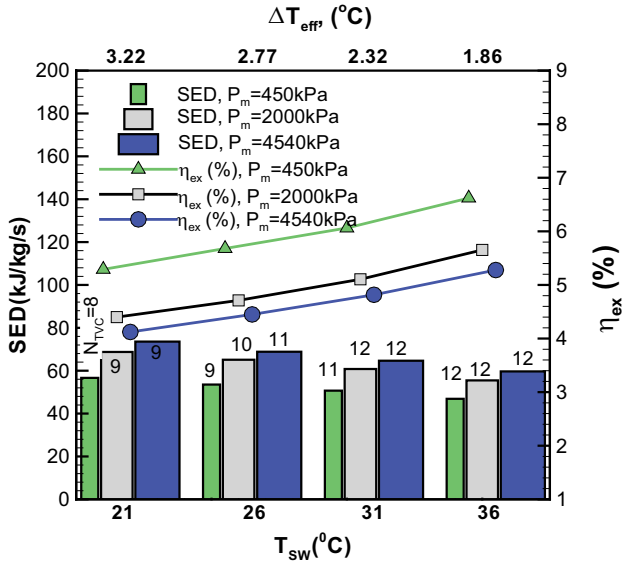

Fig. 22. Effect of cooling seawater temperature on the SED and Ex_{eff} of the system, 12 effects, T_S = 70°C.

of cooling seawater temperature also decreases the SED and consequently increases the exergy efficiency of the system as it is depicted in Fig. 22. The reason is that the TVC discharge pressure (C_r) is decreased by decreasing the temperature difference between the effects. In consequence, the irreversibilities which are caused by high C_rs would be decreased.

5. Conclusion

A thermodynamic analysis was performed on the MED/TVC desalination unit with different N_{eff}s. The calculations were done for different cooling seawater temperatures, motive steam pressures, heating steam temperatures and changing the TVC location. The following outcomes were derived from the present study:

- In MED/TVC with lower N_{eff}s, the optimal TVC location is almost the same for different motive steam pressures.
- For each N_{eff}s, the specific heat transfer area of the system at different motive steam pressures is obtained to be approximately equal to the same value if TVC is located at its optimal place.
- The entrainment ratio (Ra) changes from 0.85 to 4.25 depending on the N_{eff}s and motive steam pressures.
- The minimum specific heat transfer areas are obtained at maximum GORs. The increase in the N_{eff}s or motive steam pressure results in decreasing the specific heat transfer area.
- The exergy efficiency of the system is low at higher motive steam pressures or lower N_{eff}s. The maximum and minimum exergy efficiencies are obtained as 7.31% and 3.19%, respectively, for the system with 16 effects (P_m = 250 kPa) and 8 effects (with P_m = 4,540 kPa).
- The increasing of the heating steam temperature (T_S) from 65°C to 80°C decreases the specific heat transfer by about 94%. However, this results in increasing of the temperature difference between the effects (ΔT_{eff}), increasing the TVC discharge pressure and motive steam mass flow rate and consequently increasing the heat consumption and decreasing the GOR of the system. Also, when the T_S is increased, the irreversibility of the system is increased due to increasing the TVC discharge pressure.
- The increasing of cooling seawater temperature increases the specific heat transfer area of the system. However, the decreasing of ΔT_{eff}, which is obtained by increasing the cooling seawater temperature, causes to decrease the TVC discharge pressure and motive steam mass flow rate which consequently results in decreasing the heat consumption and increasing the GOR of the system. As a consequence, by decreasing the TVC discharge pressure, the irreversibility of the system is decreased at higher cooling seawater temperature.

Acknowledgments

This research work has been supported by University of Zabol, deputy for the research and technology, under the Grant code of UOZ-GR-9517-89.

Symbols

A_e	—	Effect heat transfer area, m²
A_f	—	Feed water preheater heat transfer area, m²
A_c	—	Condenser heat transfer area, m²
B	—	Brine water flow rate, kg/s
BF	—	Backward Feed
BPE	—	Boiling point elevation
C	—	Specific heat, kJ/kg°C
C_r	—	Compression ratio
D	—	Distillate, kg/s
D_r	—	Entrained vapor mass flow rate, kg/s
D_s	—	Motive steam mass flow rate, kg/s
E_r	—	Entrainment ratio
F	—	Feed water flow rate, kg/s
FF	—	Forward feed

GOR	—	Gain output ratio
h_d	—	Enthalpy of discharged steam, kJ/kg
h_{fd}	—	Enthalpy of discharged saturated liquid, kJ/kg
h_0	—	Enthalpy at dead state, kJ/kg
LMTD	—	Logarithmic mean temperature difference of condenser, °C
MED	—	Multi effect desalination
NEA	—	None equilibrium allowance
N_{eff}s	—	Number of effects
PCF	—	Parallel cross feed
PF	—	Parallel feed
P_d	—	Discharge vapor pressure, kPa
P_r	—	Entrained vapor pressure, kPa
P_s	—	Motive steam pressure, kPa
Q	—	Specific heat consumption, kJ/kg
Ra	—	Entrainment ratio
R_u	—	Universal constant of gases, kJ/(kmol°C)
SA	—	Specific area of MED, m²/kg/s of D
SED	—	Specific exergy destruction, kJ/(kg/s)
SHC	—	Specific heat consumption, kJ/kg
s_0	—	Entropy at dead state, kJ/kg°C
T	—	Brine temperature, °C
T_C	—	Condenser temperature, °C
T_f	—	Temperature of feed seawater, °C
T_0	—	Temperature at dead state, °C
T_{SW}	—	Seawater temperature, °C
T_v	—	Saturated vapor temperature, °C
TVC	—	Thermal vapor compression
U_e	—	Heat transfer coefficient of effect, kW/m²°C
U_f	—	Heat transfer coefficient of feed seawater preheater, kW/m²°C
U_c	—	Heat transfer coefficient of condenser, kW/m²°C
X_b	—	Salt concentration of brine, ppm
X_f	—	Salt concentration of feed water, ppm
Y	—	Flash rate in flashing boxes
η_{ex}	—	Exergy efficiency, %
λ	—	Latent heat of evaporation, kJ/kg
ΔT_{eff}	—	Temperature difference between the effects, °C
Ø	—	Dissociation factor of salt

References

[1] I. Baniasad. Askari, M. Ameri, Combined linear Fresnel solar rankine cycle with multi effect desalination (MED) process: effect of solar DNI level on the electricity and water production cost, Desal. Wat. Treat., 126 (2018) 97–115.

[2] A. Javadpour, Kh. Lari, E. Jahanshahi, I. Baniasad Askari, Techno-economic analysis of combined gas turbine, MED and RO desalination systems to produce electricity and drinkable water, Desal. Wat. Treat., 159 (2019) 232–249.

[3] Sh. Gorjian, B. Ghobadian. Solar desalination: a sustainable solution to water crisis in Iran, Renew. Sustain. Energy Rev., 48 (2015) 571–584.

[4] I. Baniasad Askari, M. Ameri, F. Calise, Energy, exergy and exergo-economic analysis of different water desalination technologies powered by linear Fresnel solar field, Desalination, 428 (2018) 37–67.

[5] S.M. Alelyan, N.W. Fette, E.B. Stechel, P. Doron, P.E. Phelan, Techno-economic analysis of combined ammonia-water absorption refrigeration and desalination, Energy Convers. Manage., 143 (2017) 493–504.

[6] I. Janghorban Esfahani, Ch. Yoo, A highly efficient combined multi-effect evaporation-absorption heat pump and vapor-compression refrigeration part2: Thermo economic and flexibility analysis, Energy, 75 (2014) 327–337.

[7] Z.M. Amin, M.N.A. Hawlader, Analysis of solar desalination system using heat pump, Renew. Energy, 74 (2015) 116–123.

[8] I. Baniasad Askari, M. Ameri, The application of Linear Fresnel and Parabolic Trough solar fields as thermal source to produce electricity and fresh water, Desalination, 415 (2017) 90–103.

[9] I. Baniasad Askari, M. Ameri, Solar Rankin cycle (SRC) powered by linear Fresnel solar field and integrated with combined MED desalination system, Renew. Energy, 117 (2018) 52–70.

[10] A. Tamburini, A. Cipollina, G. Micale, A. Piacentino, CHP (combined heat and power) retrofit for a large MED-TVC (multiple effect distillation along with thermal vapour compression) desalination plant: high efficiency assessment for different design options under the current legislative EU framework, Energy, 115 (2016) 1548–155.

[11] I. Baniasad Askari, M. Ameri, M. Technoeconomic feasibility analysis of MED/TVC desalination unit powered by linear Fresnel solar field direct steam, Desalination, 394 (2016) 1–17.

[12] P. Catrini, A. Cipollina G. Micale, A. Piacentino, A. Tamburini, Exergy analysis and thermoeconomic cost accounting of a combined heat and power steam cycle integrated with a multi effect distillation-thermal vapour compression desalination plant, Energy Convers. Manage., 149 (2017) 950–965.

[13] A. Kouta, G. Al-Sulaima, M. Atif, S. Bin Marshad, Entropy, exergy, and cost analyses of solar driven cogeneration systems using supercritical CO_2 Brayton cycles and MEE-TVC desalination system, Energy Convers. Manage., 115 (2016) 253–264.

[14] A.O. Bin Amer, Development and optimization of ME-TVC desalination system, Desalination, 249 (2009) 1315–1331.

[15] I.S. Al-Mutaz, I. Wazeer, Development of a steady-state mathematical model for MEE-TVC desalination plants, Desalination, 351 (2014) 9–18.

[16] F.N. Alasfour, M.N. Darwish, A.O. Bin Amer, Thermal analysis of ME-TVC+MEE desalination systems, Desalination, 174 (2005) 39–61.

[17] B. Ortega-Delgado, P. Palenzuela, D.C. Alarcón-Padilla, Parametric study of a multi-effect distillation plant with thermal vapor compression for its integration in to a Rankine cycle power block, Desalination, 394 (2016) 18–29.

[18] R. Kouhikamali, M. Sanaei, M. Mehdizadeh, Process investigation of different locations of thermo-compressor suction in MED-TVC plants, Desalination, 280 (2011) 134–138.

[19] H. Fathia, Kh. Tahar, B.Y. Ali, B.B. Ammar, Exergoeconomic optimization of a double effect desalination unit used in an industrial steam power plant, Desalination, 438 (2018) 63–82.

[20] K. Khalid, M. Antar, A. Khalifa, O. Hamed, Allocation of thermal vapor compressor in multi-effect desalination systems with different feed configurations, Desalination, 426 (2018) 164–173.

[21] M.L. Elsayed, O. Mesalhy, R.H. Mohammed, L.C. Chow, Exergy and thermo-economic analysis for MED-TVC desalination systems, Desalination, 447 (2018) 29–42.

[22] R. Kouhikamali, Thermodynamic analysis of feed water pre-heaters in multiple effect distillation systems, Appl. Thermal Eng., 50 (2013) 1157–1163.

[23] M.L. Elsayed, O. Mesalhya, R.H. Mohammed, L.C. Chow, Effect of input parameters intensity and duration on dynamic performance of MED-TVC Plant, Appl. Thermal Eng., 137 (2018) 475–486.

[24] M.H. Sharqawy, J.H. Lienhard, S.M. Zubair, Thermophysical properties of seawater: a review of existing correlations and data. Desal. Wat. Treat., 16 (2010) 354–380.

[25] A.S. Hassan, M.A. Darwish, Performance of thermal vapor compression, Desalination, 35 (2014) 41–46.

[26] F. Calise. M.D. d›Accadia. A. Piacentino, Exergetic and exergoeconomic analysis of a renewable polygeneration system and viability study for small isolated communities, Energy, 92 (2015) 290–307.

[27] F. Calise, M.D. d'Accadia, A. Macaluso, A. Piacentino, L. Vanoli, Exergetic and exergoeconomic analysis of a novel hybrid solar–geothermal polygeneration system producing energy and water, Energy Convers. Manage., 115 (2016) 200–220.
[28] Fichtner (Fichtner GmbH & Co. KG) and DLR (Deutsches Zentrum für Luft und Raumfahrt e.V.), MENA Regional Water Outlook, Part II, Desalination Using Renewable Energy, Task 1–Desalination Potential; Task 2–Energy Requirements; Task 3–Concentrate Management. 2011, available at: http://www.dlr.de/tt/Portaldata/41/Resources/dokumente/institut/system/projects/MENA_REGIONAL_WATER_OUTLOOK.pdf.